

## Subgrid-scale modeling of reacting scalar fluxes in large-eddy simulations of atmospheric boundary layers

J.-F. Vinuesa<sup>1?</sup>, F. Porte-Agel<sup>1,2</sup>, S. Basu<sup>1</sup>, R. Stoll<sup>1</sup>

<sup>1</sup> Saint Anthony Falls Laboratory and Department of Civil Engineering, University of Minnesota, Minneapolis, United States of America

<sup>2</sup> National Center for Earth-surface Dynamics

Submitted: June 17, 2005

**Abstract** In large-eddy simulations of atmospheric boundary layer turbulence, the lumped coefficient in the eddy-diffusion subgrid-scale (SGS) model is known to depend on scale for the case of inert scalars. This scale dependence is predominant near the surface. In this paper, a scale-dependent dynamic SGS model for the turbulent transport of reacting scalars is implemented in large-eddy simulations of a neutral boundary layer. Since the model coefficient is computed dynamically from the dynamics of the resolved scales, the simulations are free from any parameter tuning. A set of chemical cases representative of various turbulent reacting flow regimes is examined. The reactants are involved in a first-order reaction and are injected in the atmospheric boundary layer with a constant and uniform surface flux. Emphasis is placed on studying the combined effects of resolution and chemical regime on the performance of the SGS model. Simulations with the scale-dependent dynamic model yield the expected trends of the coefficients as function of resolution, position in the flow and chemical regime, leading to resolution-independent turbulent reactant fluxes.

**Key words** Large-eddy simulation { Subgrid-scale models { Turbulent transport { Atmospheric chemistry { Atmospheric boundary layers

**Abbreviations** ABL - Atmospheric boundary layer; LES - Large-eddy simulation; SGS - Subgrid scale; RANS - Reynolds Averaged Navier Stokes

---

<sup>?</sup> Corresponding address: J.-F. Vinuesa, Saint Anthony Falls Laboratory, Mississippi river at 3rd Avenue SE, Minneapolis, MN 55414, USA, e-mail: vinue001@umn.edu

## 1 Introduction

The atmospheric boundary layer (ABL) is the lower part of the atmosphere, where turbulence plays an essential role on the transport of momentum and scalars (heat, water vapor and chemicals) between the biosphere and the upper atmosphere. Quantifying the transport rate of chemicals from the Earth's surface into the upper parts of the atmosphere is critical for a wide range of environmental applications, including air quality modeling and regional and global climate studies. One important open question is how to represent the effects of boundary layer physical processes, in particular turbulence, on chemical transport and transformation of chemical compounds. A large number of reactive gases emitted by vegetation, such as biogenic volatile organic compounds, have typical lifetimes that are of the same order of magnitude or smaller than the mixing time scales of the largest ABL eddy motions [1]. For such species (isoprene and monoterpenes for instance) the interplay between turbulence and chemistry is of great importance. Accurate modeling of their chemical transformations in the ABL requires improved understanding on how turbulence and spatial distribution of the reactants affect chemistry.

Realistic numerical experiments on the turbulent transport and mixing of reactants require the use of Large-Eddy Simulation (LES). In the atmospheric boundary layer, the scales associated with turbulent motions range from the Kolmogorov dissipation scale (on the order of a millimeter) to the boundary layer depth (on the order of a kilometer). The largest eddies are responsible for the turbulent transport of the scalars and momentum whereas the smallest ones are mainly dissipative. LES consists of explicitly resolving all scales larger than the grid scale (on the order of tens of meters in the ABL), while the smallest (less energetic) scales are parameterized using a subgrid-scale (SGS) model. Since the pioneering paper of Schumann [2] that showed for the first time that segregation of reactants due to inefficient mixing of the convective turbulence plays an important role on moderating the reaction rates, several numerical studies on the effect of turbulence on chemistry in the ABL have been performed using LES [3,4,5,6,7,8,9,10,11,12,13,14,15,16,17]. In particular, Gao et al. [3] and Patton et al. [14] focused their study on the lowest part of the ABL and on the interplay between chemistry and turbulence in and above canopies.

An important challenge in large-eddy simulations of the atmospheric boundary layer is the specification of the SGS model coefficients and, in particular, how to account for external or internal parameters such as position in the flow, grid/filter scale, atmospheric stability and chemical regime. Usually in LES of atmospheric turbulent reacting flows, the subgrid reactant flux is modeled as the product of a local gradient of the concentrations from the resolved scales and of eddy-diffusivity coefficients. These coefficients are either simply prescribed (in the case of Smagorinsky models) or estimated by solving an equation for the turbulent kinetic energy assuming that subgrid scale turbulence is equally efficient at transporting scalars as it is for

heat [18]. In this paper, we explicitly calculate the model coefficients by using a dynamic procedure and without making any assumption of the ability of subgrid turbulence to transport scalars. Thus the model coefficients are specifically calculated for each reacting scalar.

When studying the effects of the unresolved scales on the chemical transformations, e.g. related to the subgrid scale mixing between the reactants due to subgrid scale turbulence, Vinuesa and Porte-Agel [19] suggest that these effects can be correlated with the chemical regime. Since the SGS reactant flux includes a chemical contribution in its governing equation, chemical regime dependency of the subgrid scale transport can be also expected. By using a set of chemical setups representative of several chemical regimes, one can study the relevance of this chemical dependency of the reactant subgrid fluxes.

Recently, Porte-Agel [20] showed that the lumped coefficient used in the eddy-diffusion models for inert scalars are strongly scale dependent, in particular close to the surface. In order to account for that scale dependence of the coefficient, he developed a scale-dependent dynamic procedure to compute the value of the eddy-diffusion coefficient using information contained in the resolved scales. In this paper, we use this tuning-free scale-dependent dynamic model for simulations of reacting scalars.

The structure of this paper is as follows. In section 2, we present a scale-dependent dynamic model for the turbulent transport of reactants in the ABL. The model is used for simulations of a neutral atmospheric boundary layer. The characteristics of the simulations are presented in section 3. A set of simulations is performed in order to study the combined effects of chemical regime and resolution. The relative importance of subgrid-scale turbulence on the chemistry is classified using a subgrid-scale Damköhler number. By focusing our analysis on a first order decaying scalar, we are able to isolate the effects of the unresolved scales on the turbulent transport of the reactants. Emphasis is placed on the scale-independence of the simulated reactant fluxes and on the combined effects of chemical regime and resolution on the dynamically computed model coefficients and scale-dependence parameters. Finally, conclusions are drawn in section 2.

## 2 The scale-dependent dynamic model

The filtered governing equation for the concentration of a reacting scalar  $A$  that is solved in LES reads:

$$\frac{\partial \bar{c}_A}{\partial t} + \mathbf{a}_i \frac{\partial \bar{c}_A}{\partial x_i} = \frac{\partial u_i^{(0,0)} c_A^{(0,0)}}{\partial x_i} + \mathcal{R}_{\text{ch}} \quad (1)$$

where  $\bar{c}_A$  and  $c_A^{(0,0)}$  are the spatially filtered (at the filter scale  $\Delta$ ) and the subgrid concentrations of the reactant, respectively.  $u_i^{(0,0)}$  is the subgrid-scale flux and  $\mathcal{R}_{\text{ch}}$  is the chemical term. For a reactant  $A$  involved in the first-order reaction

$$\mathbf{A} = \mathbf{A}^j \text{ Products}; \quad (2)$$

the chemical term reads

$$\mathbb{R}_{\text{ch}} = \mathbf{j} \mathbf{c}_A; \quad (3)$$

The effect of the unresolved scales on the evolution of the filtered scalar concentration appears through the subgrid scale reactant flux

$$\mathbb{J}_i^{\text{sgs}} c_A^{\text{sgs}} = \mathbf{u}_i c_A - \mathbf{e}_i \mathbf{c}_A; \quad (4)$$

It is important to note that in the case of a second-order reaction (not considered here), the unresolved scales can affect the reactant concentrations not only through the subgrid-scale fluxes but also through the subgrid-scale covariances (see e.g. [21,19]).

The subgrid reactant flux is usually modeled as a function of a local gradient of the resolved concentrations using an eddy-diffusivity model. The subgrid-scale Schmidt number in that model is either simply prescribed as a constant value or estimated assuming that subgrid scale turbulence is equally efficient at transporting reacting scalars as it is for heat.

The eddy-diffusion subgrid model is widely used in LES of the atmospheric boundary layer. A common formulation of this model for the subgrid scale flux of a scalar is

$$\mathbb{J}_i^{\text{sgs}} c_A^{\text{sgs}} = -\frac{1}{Sc_{\text{sgs}}} \mathcal{S}_{ij} \frac{\partial c_A}{\partial x_j}; \quad (5)$$

where  $\mathcal{S}_{ij} = (2\mathcal{S}_{ij}\mathcal{S}_{ij})^{1/2}$  is the resolved strain-rate magnitude,  $\mathcal{S}_{ij}$  is the resolved strain rate tensor,  $\ell$  is the filter scale and  $c_A$  is the resolved (spatially filtered) scalar concentration.  $Sc_S$  and  $Sc_{\text{sgs}}$  denote the Smagorinsky coefficient in the eddy-viscosity model and the subgrid-scale Schmidt number for the scalar  $\phi$ , respectively.

Usually the subgrid-scale Schmidt number  $Sc_{\text{sgs}}$  and, as a consequence, the lumped coefficient  $Sc_{\text{sgs}}^{-1} Sc_S^2$  are only determined (calculated or prescribed) for inert scalars, and those values are used for the calculation of the subgrid scale reactant fluxes using Equation (5). It is, therefore, assumed that chemistry does not affect the subgrid scale fluxes and, consequently,  $Sc_{\text{sgs}}^{\text{chem}} = Sc_{\text{sgs}}$ , where  $Sc_{\text{sgs}}$  is the subgrid-scale Schmidt number for an inert scalar.  $Sc_{\text{sgs}}$  is often taken as a constant value ( $Sc_{\text{sgs}} = 1/3$ ), which is well-established for isotropic turbulence [22,23]. However, near the surface of ABL flows, the reacting scalar field at the smallest resolved scales can become anisotropic due to the combined effects of proximity to the surface, resolution (filter/grid scale), atmospheric stability and/or chemical regime. In the following, we propose an alternative procedure to calculate the value of the lumped eddy-diffusion model coefficient that is able to adjust to the

anisotropy of the reacting scalar field associated with the aforementioned factors. In particular, the value of the lumped model parameter  $Sc_{sgs}^{-1} C_S^2$  is determined based on the dynamics of the smallest resolved scales using the scale-dependent dynamic model introduced for passive scalars by Porte-Agel [20]. This tuning-free procedure is summarized below.

For the reactant subgrid scale flux  $u_{i,j}^{0,0}$  (denoted  $q_{A,j}$  hereafter to enhance readability), the dynamic procedure is based on the Germano identity for scalars [24,25]

$$K_{A,j} = Q_{A,j} - \overline{q_{A,j}} = \overline{u_i \phi_A} - \overline{u_i} \overline{\phi_A}; \quad (6)$$

where  $Q_{A,j} = \overline{u_i \phi_A} - \overline{u_i} \overline{\phi_A}$  is the subgrid scale flux at a test-filter scale (typically taken as  $\overline{\cdot} = 2$ ) and  $K_{A,j}$  is a resolved reactant flux that can be evaluated based on the resolved scales. Applying the eddy-diffusion model,  $Q_{A,j}$  is determined by

$$Q_{A,j} = - \frac{h}{Sc_{sgs;A}^{-1} C_S^2} \overline{u_i} \frac{\partial \overline{\phi_A}}{\partial x_i}; \quad (7)$$

Substitution of Equations (5) and (7) into (6) leads to the system

$$K_{A,j} = Sc_{sgs;A}^{-1} C_S^2 X_{A,j}; \quad (8)$$

where, for  $\overline{\cdot} = 2$ ,

$$X_{A,j} = - \frac{2}{Sc_{sgs;A}^{-1} C_S^2} \overline{u_i} \frac{\partial \overline{\phi_A}}{\partial x_i} - 4 \frac{Sc_{sgs;A}^{-1} C_S^2 (2)}{Sc_{sgs;A}^{-1} C_S^2 (\cdot)} \overline{u_i} \frac{\partial \overline{\phi_A}}{\partial x_i}; \quad (9)$$

Note that the traditional dynamic model [20] assumes scale invariance of the model coefficient at the filter and test-filter scales, i.e.,

$$Sc_{sgs;A}^{-1} C_S^2 (\cdot) = Sc_{sgs;A}^{-1} C_S^2 (2) = Sc_{sgs;A}^{-1} C_S^2; \quad (10)$$

Minimizing the error associated with the use of the eddy-diffusion model in Equation (6) over all three vector components results in

$$Sc_{sgs;A}^{-1} C_S^2 (\cdot) = \frac{h K_{A,j} X_{A,j}^i}{h X_{A,j} X_{A,j}^i}; \quad (11)$$

where  $h$  denotes an averaging operator (typically over horizontal planes) and  $X_{A,j}$  contains the scale-dependent parameter  $\overline{\beta}_A = \frac{Sc_{sgs;A}^{-1} C_S^2 (2)}{Sc_{sgs;A}^{-1} C_S^2 (\cdot)}$ . Please note that  $\overline{\beta}_A = 1$  in the case of the traditional dynamic model. A dynamic procedure can be developed to compute the value for  $\overline{\beta}_A$  using a second test-filtering operation at scale  $\overline{\beta} > 4$ . For the sake of simplicity, we take a second test-filter scale as  $\overline{\beta} = 4$ , and denote variables filtered at scale 4 by a caret. This results in a second equation for  $Sc_{sgs;A}^{-1} C_S^2 (\cdot)$  that reads

$$Sc_{sgs;A}^{-1} C_S^2(\cdot) = \frac{K_{A;i}^0 X_{A;i}^0}{X_{A;i}^0 X_{A;i}^0}; \quad (12)$$

where

$$K_{A;i}^0 = \frac{d}{dx_i} \frac{b_i}{c_i}; \quad (13)$$

and

$$X_{A;i}^0 = \frac{\partial c_i}{\partial x_i} \frac{Sc_{sgs;A}^{-1} C_S^2(\cdot)}{Sc_{sgs;A}^{-1} C_S^2(\cdot)} \frac{d}{dx_i} \frac{b_i}{c_i}; \quad (14)$$

By combining Equations 11 and 12, one obtains the following equation from which  $\alpha_A$  can be computed (more details on this procedure are given in Porte-Agel [20]),

$$hK_{A;i}^0 X_{A;i}^0 X_{A;i}^0 X_{A;i}^0 - K_{A;i}^0 X_{A;i}^0 hX_{A;i}^0 X_{A;i}^0 = 0; \quad (15)$$

The value of  $\alpha_A$  is extracted from Equation 15 assuming that

$$\frac{Sc_{sgs;A}^{-1} C_S^2(\cdot)}{Sc_{sgs;A}^{-1} C_S^2(\cdot)} = \frac{Sc_{sgs;A}^{-1} C_S^2(\cdot)}{Sc_{sgs;A}^{-1} C_S^2(\cdot)} \quad (16)$$

which implies that  $Sc_{sgs;A}^{-1} C_S^2(\cdot) = Sc_{sgs;A}^{-1} C_S^2(\cdot) = \frac{2}{\alpha_A}$ .

Then  $\alpha_A$  is used in Equation 11 to obtain the lumped coefficient  $Sc_{sgs;A}^{-1} C_S^2$ .

### 3 Reacting atmospheric flow simulations

#### 3.1 Turbulent reacting flow classification

Turbulent reacting flows can be classified by using two dimensionless numbers [2,26]. The first one, i.e. the turbulent integral Damkohler number,  $Da_t$ , refers to the influence of the largest atmospheric boundary layer eddies on reacting scalars. In the context of Reynolds Averaged Navier Stokes (RANS) modeling, it gives a measure of the relative importance of the dynamical and chemical contributions to the reacting scalar mean governing equation. The second number, i.e. the Kolmogorov Damkohler number,  $Da_k$ , quantifies the relative magnitude of the characteristic time scales of the smallest ABL eddies with respect to the chemical reaction time scale. These numbers are defined as

$$Da_t = \frac{t}{c}; \quad (17)$$

$$Da_k = \frac{k}{c}; \quad (18)$$

where  $\tau_t$  is the integral turbulent time scale,  $\tau_k$  is the Kolmogorov time scale and  $\tau_c$  is the chemical time scale.

Using these Damkohler numbers, the following classification of chemical regime in turbulent reacting flows can be made:

- {  $Da_t < 1$ , slow chemical regime: the reactant is uniformly mixed in the boundary layer and its governing equation is dominated by the dynamical terms.
- {  $Da_k < 1 < Da_t$ , moderate chemical regime: the largest scales affect the turbulent mixing whereas the chemistry is not limited by the smallest-scale turbulence.
- {  $Da_k > 1$ , fast chemical regime: turbulence controls the chemistry at all scales.

In the context of large-eddy simulation, it is also very important to assess the effects of the subgrid scales on chemistry. In order to achieve that, it is convenient to introduce the so-called subgrid Damkohler number or  $Da_{sgs}$  [11]

$$Da_{sgs} = \frac{\tau_{sgs}}{\tau_c}; \quad (19)$$

$Da_{sgs}$  is a measure of the relative magnitude of the time scale associated with the smallest eddies resolved in LES with respect to the chemical time scale. That time scale can be computed as

$$\tau_{sgs} = \frac{\nu_{sgs}^{1/2}}{\epsilon_{sgs}}; \quad (20)$$

where  $\nu_{sgs}$  and  $\epsilon_{sgs}$  are the subgrid-scale eddy viscosity and the subgrid-scale dissipation rate of the turbulent kinetic energy, respectively. The subgrid-scale dissipation rate is defined as the rate of transfer of kinetic energy between the resolved and the subgrid scales [27,28]. By using  $Da_{sgs}$ , turbulent reacting flows are classified with respect to the effect of the unresolved scales on the chemistry. For  $Da_{sgs} \ll 1$ , the flow is well-mixed at subgrid scales and, consequently, the unresolved scales do not influence the behavior of reacting scalars. For  $Da_{sgs} \sim O(1)$  and  $> 1$ , all the scales of turbulence, i.e. resolved and subgrid, affect the chemistry. These effects on the transport and mixing of reactants lead to a heterogeneous distribution of the reactants at subgrid scales.

### 3.2 Numerical set-up

The code used is a modified version of 3-dimensional LES code described by Albertson and Parlange [29], Porte-Agel et al. [30], and Porte-Agel [20]. Briefly, the code uses a mixed pseudospectral finite-difference method and the subgrid-scale stresses and momentum and temperature fluxes are parameterized with scale-dependent dynamic models. Test filtering for dynamic

models is done using two-dimensional spectral cut-off filters. A chemical solver has been implemented in the LES code [19]. We simulate a neutral atmospheric boundary layer driven by a pressure gradient forcing and a surface roughness length form on momentum of 0.1m is prescribed. The computational domain is of size  $(L_x, L_y, L_z)$  and it correspond to a grid prescribed with  $N \times N \times N$  points. The height of the domain  $L_z$  is equal to 1000 meters and  $L_x = L_y = 2 L_z$ . Several resolutions are used with  $N$  equal to 32, 64, and 128.

In order to restrict our study to the performance of the scale dependent subgrid-scale model for the reactant flux, the studied reacting flow consists of the first-order reaction (2).

We define three chemical setups based on this first-order irreversible reaction. The reactant A, so-called bottom-up reactant, is uniformly emitted at the surface with a flux of  $0.1 \text{ ppb m s}^{-1}$  and no initial concentrations in the boundary layer. The reaction rate  $j$  is set to zero,  $4.5 \times 10^{-4} \text{ s}^{-1}$ , and  $9 \times 10^{-3} \text{ s}^{-1}$ . The corresponding chemical set-up will be refer to as inert (I), slow (S) and fast (F) chemical cases. Notice that, in our simulations,  $\tau_c = h/u$  and  $\tau_c = j^{-1}$  lead to turbulent Damkohler numbers  $Da_\tau$  equals to 0, 1 and 20, respectively. The simulations cover a 1.5 hours period and the statistics presented here are obtained averaging the results over the last hour of simulation.

### 3.3 Results

In Fig. 1, the vertical profiles of the subgrid scale Damkohler number  $Da_{sgs}$  are shown. For the slow (S) chemical regime, the chemical time scale ( $\tau_c$ ) is much larger than the characteristic subgrid-scale time scale ( $\tau_{sgs}$ ), which determines a relatively small value of  $Da_{sgs}$  for all resolutions. On the contrary, all the fast (F) chemical cases have  $Da_{sgs} \gg 1$  and, as a result, the transport of the reacting scalar is affected by the subgrid scale chemistry. The value of  $Da_{sgs}$  and, consequently, the effect of the subgrid-scale chemistry on the scalar fluxes, increases with decreasing resolution due to the fact that the characteristic time scale of the subgrid fluxes is larger for coarser grids.

Fig. 2 shows the vertical profiles of the time-averaged total scalar fluxes obtained as the sum of the resolved and the subgrid-scale fluxes. Within the boundary layer, the profiles of inert scalar fluxes have a linear shape. As noticed by Porte-Agel [20], since a constant mean surface flux is imposed and no viscous effects are considered, the averaged total turbulent flux decreases linearly with height. The reactive scalar flux profiles, however, deviate from this linear behavior. In fact, these deviations become more significant when the turbulent Damkohler number increases; they are larger for the F experiment than for the S one. The deviations increase with the reaction rate and, thus, with the turbulent Damkohler number due to the increase in the chemical contribution to the flux. This was shown also by Gao and We-

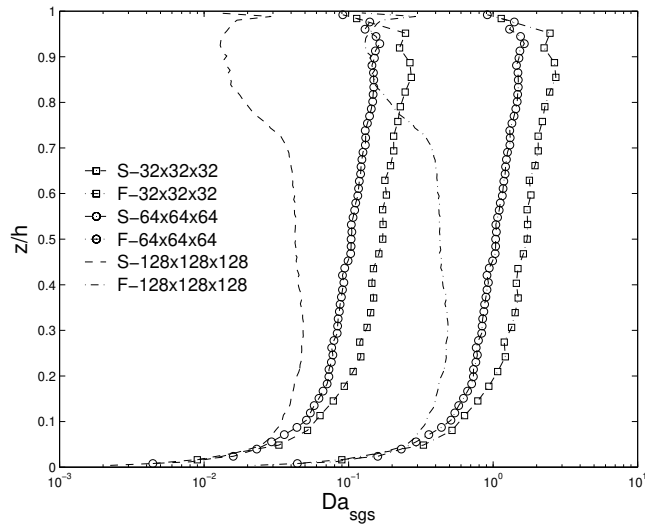


Fig. 1 Vertical profiles of the subgrid scale Damkohler numbers. These numbers have been obtained dynamically and averaged over the last hour of simulation. The S and F chemical cases are represented by dashed and dash-dotted lines, respectively, and the  $32^3$ ,  $64^3$  and  $128^3$  grid-points simulations are plotted with squares, circles and no symbol, respectively.

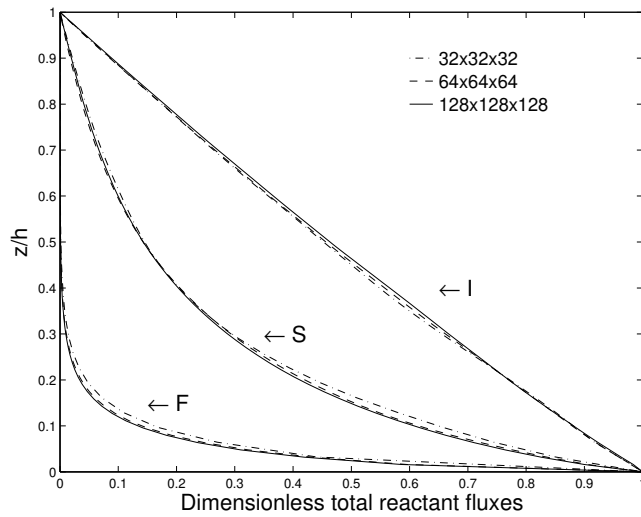


Fig. 2 Vertical profiles of the total scalar fluxes averaged over the last hour of simulation. Results are made dimensionless by using the surface fluxes.

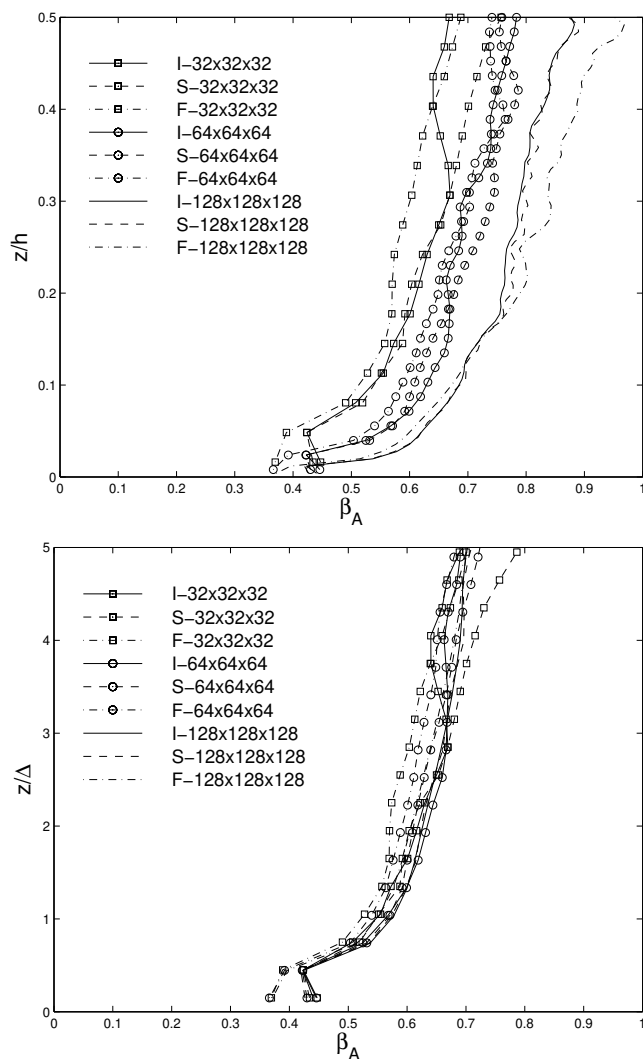


Fig. 3 Vertical profiles of  $\beta_A$  as a function of the height made dimensionless using the boundary layer depth  $h$  (upper figure) and the filter size (lower figure). The results have been averaged over the last hour of simulation.

sely [5], Sykes et al. [4], and V inuesa and Vila-Guerau de Arellano [15] for convective boundary layers.

As mentioned earlier, the magnitude of the subgrid-scale fluxes are affected by both the resolution and the chemical regime. The fact that the total turbulent fluxes (resolved plus subgrid contributions) for each chemical regime show almost identical results for the three resolutions under consideration highlights the robustness of the scale-dependent dynamic model. This subgrid model is able to adjust the magnitude of the subgrid-scale

fluxes to yield the same total turbulent fluxes. It is important to note that the resolution independence of the results is one of the most challenging tests for any subgrid-scale model, especially when the subgrid-scale effects are also affected by the chemical regime.

The time-averaged values of the scale-dependence parameter  $\alpha_A$  are shown in Fig. 3 as a function of the normalized heights  $z=h$  and  $z=0.5$ .  $\alpha_A$  is smaller near the surface, indicating a strong scale dependence in that region, and it increases to larger values far from the surface. Note, however, that the scale-dependence coefficients obtained far from the surface are still slightly smaller than the value of 1, indicating a slight scale dependence and flow anisotropy. This behavior contrasts with the value of 1 obtained for the scale-dependent parameter for the momentum fluxes as reported by Porte-Agel [20], and it could be attributed to the more anisotropic behavior of scalars (compared with the velocity field) in turbulent flows. From Fig. 3, it is also clear that  $\alpha_A$  depends on both resolution (scale  $\Delta$ ) and chemical regime (characterized by the subgrid Damköhler number). The scale dependence of  $\alpha_A$  was already demonstrated by Porte-Agel [20] for the case of an inert scalar, by showing that the values of  $\alpha_A$  computed at different resolutions collapse when plotted against  $z=0.5$ . The fact that in our simulations the collapse of the curves is not perfect is due to the additional effect of chemistry on the subgrid-scale fluxes. This effect is further explored below.

Fig. 4 shows the vertical profiles of scale-dependent parameter  $\alpha_A$  and the lumped coefficient  $Sc_{sgs,A}^{-1} C_S^2$  as a function of the normalized height  $z=0.5$ . In order to isolate the effect of the chemical regime from that of the resolution, the results from each resolution are presented in different panels. One can notice that for both  $\alpha_A$  and  $Sc_{sgs,A}^{-1} C_S^2$ , the results from the inert and slow chemical cases are the same for the highest resolution. They are not affected by the chemistry in the I and S chemical cases, showing only a scale (resolution) dependence. The little effect of the chemistry on the subgrid fluxes in the slow chemical regime is due to the fact that the characteristic time scale of the chemistry is much larger than the characteristic time scale of the subgrid scale fluxes, as illustrated by the very low values of the subgrid Damköhler number. When decreasing (coarsening) the resolution, however, chemistry has a relatively more important effect on the subgrid-scale fluxes, which translates also into an increase in the subgrid Damköhler number. As a result, the deviation from the I chemical case profiles increases when coarsening the resolution. Chemistry has a clear effect on all F experiments with this effect increasing as the resolution coarsens and, consequently,  $Da_{sgs}$  increases. In summary, our results show that the scale-dependent dynamic model is able to capture the dependence of the subgrid coefficient and scale-dependent parameter on both resolution and chemical regime.

The scalar variance spectra of the reactive scalar obtained from all the simulations at a height of  $z = 0.3h$  are shown in Fig. 5. The spectra are calculated from spatial information using one-dimensional Fourier transforms that are then averaged in the spanwise direction and also in time. They

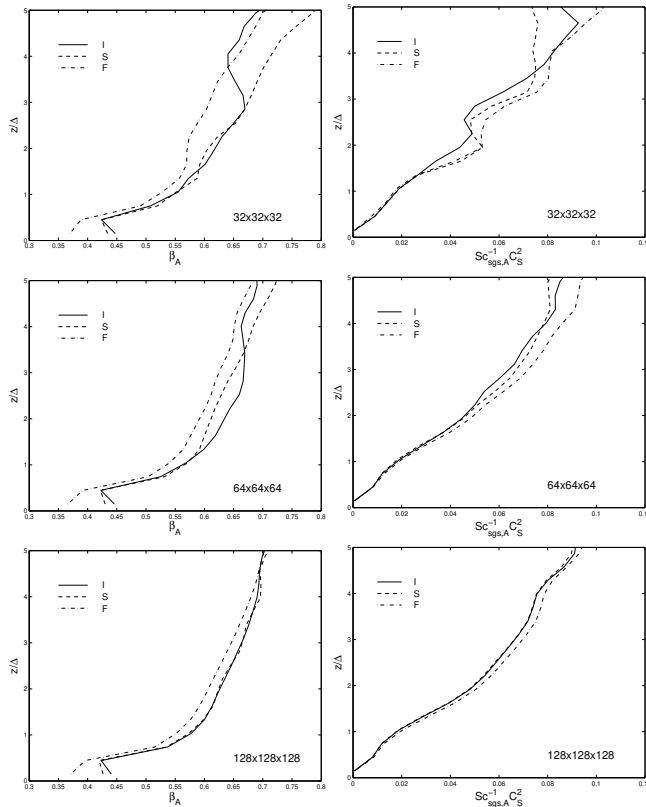


Fig. 4 Vertical profiles of  $\beta_A$  (left column) and lumped coefficient  $Sc_{sgs;A}^{-1} C_S^2$  (right column) for the  $32^3$  (upper row),  $64^3$  (middle row) and  $128^3$  (lower row) simulations. The results have been averaged over the last hour of simulation.

are normalized with  $\int_0^z \beta_A dz$ , where  $\int_0^z \beta_A dz$  is the area below the spectral curve, and they are plotted against  $k_1 z$ , where  $k_1$  is the streamwise wavenumber. Doing so allows us to focus on the distribution of the variance over the range of resolved scales. [20] showed that the normalized spectra for inert scalars and heights  $z \geq 0.3h$  collapse and are proportional to  $k_1^{-5/3}$  in the inertial subrange, which corresponds to scales smaller than the height (i.e.,  $k_1 z \ll 1$ ). At the largest scales (small wavenumbers), our results agree with Jonker et al. [16], who showed that the effect of the chemistry on the variance spectra depends on the chemical regime, characterized by the turbulent Damköhler number  $Da_t$ . For slow chemical regimes, where  $Da_t \ll 1$ , the time scale of the chemistry ( $\tau_c$ ) is much slower than the integral time scale of the turbulence ( $\tau_t$ ) and, consequently, the chemical reaction has practically no effect on the scalar variance at any of the turbulence scales. When  $Da_t \gg 0(1)$ , the chemistry is faster than the characteristic turning time of the largest eddies, which has an impact (reduction) on the level of fluctuations of the

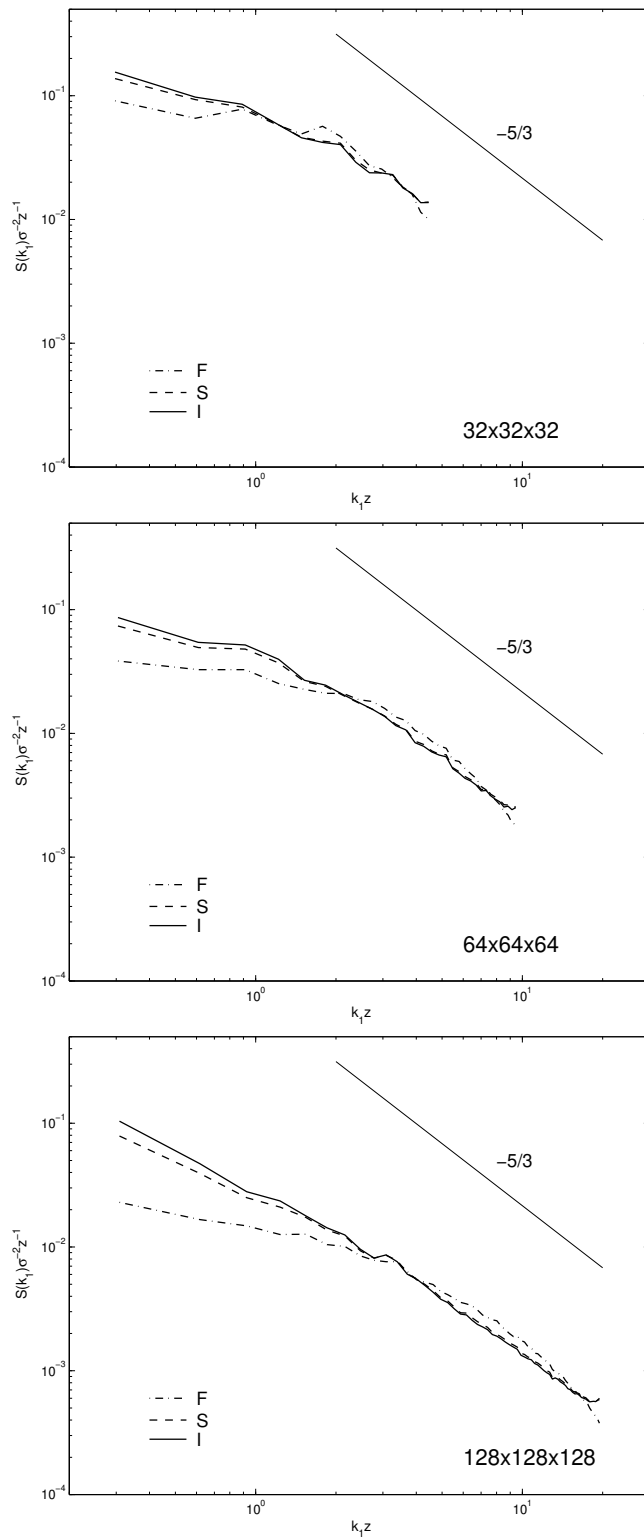


Fig. 5 Spatial variance spectra obtained for the  $32^3$ ,  $64^3$  and  $128^3$  experiments (from top to bottom), normalized by  $\rho^{-2} z$ , where  $\rho^{-2}$  is the area below the spectral curve, calculated for a height  $z = 0.3h$ . The I, S and F chemical cases are represented by solid, dashed and dash-dotted lines, respectively. The slope of  $-5/3$  is also shown.

reacting scalars at those scales. As a consequence, in Fig. 5 the spectra corresponding to the fast chemical regime show substantially smaller variance at the largest scales (small  $k_1$ ) for all the resolutions. In order to understand if that effect will extend to the subgrid and/or smallest resolved scales, one needs to consider, in addition, the value of the subgrid Damköhler number  $Da_{sgs}$ . If  $Da_{sgs} \ll 1$  then the subgrid and smallest resolved scales are not affected and, consequently, the scale-dependent dynamic model parameters are not expected to depart from the inert scalar values, as shown in Fig. 4. On the other hand, if  $Da_{sgs} \approx O(1)$ , then the effect of the chemistry extends also to the subgrid and/or smallest resolved scales, which become less isotropic. It is important to note that the tuning-free dynamic model adjusts to the less isotropic behavior of those scales through a reduction of the model parameters as shown in Fig. 4.

#### 4 Summary

A scale-dependent dynamic model for the subgrid-scale fluxes of reacting scalars is presented and used in large-eddy simulations of atmospheric boundary layer reacting flows. This model uses a dynamic procedure to calculate the lumped coefficient ( $Sc_{sgs}^{-1}; C_S^2$ ) in the eddy-diffusion subgrid-scale model as a function of the dynamics of the resolved scales. Consequently, the proposed dynamic model does not require any parameter specification or a priori tuning.

The scale-dependent dynamic model is implemented in simulations of a neutral ABL with a constant and uniform surface flux of a first-order decaying scalar. A set of spatial resolutions and reaction rates are used in order to study the ability of the dynamic model to adjust the model coefficient to changes in scale (resolution) and/or chemical regime. The model is able to account for the scale dependence of the model coefficient in a self-consistent way. Scale dependence increases with decreasing height-to-scale ratio due to the increased flow anisotropy at the filter and/or test filter scales. In addition, we found that when the time scale associated with the subgrid turbulence is on the same order of magnitude that the time scale associated with the chemistry, i.e.  $Da_{sgs} \approx O(1)$ , an additional dependence towards the chemical reactivity can be expected. By calculating explicitly the lumped model coefficients for the reacting scalars, there is no need for any assumption on the combined effects of resolution and reaction rate on the efficiency of the subgrid scale turbulence to transport scalars. We showed that the model is able to capture the chemical regime dependence of the reactant and, as a result, simulations yield resolution-independent total turbulent reactant fluxes.

**Acknowledgements** The authors gratefully acknowledge the financial support by NASA (NAG 5-11801), the National Science Foundation (EAR-0094200 and EAR-0120914 as part of the National Center for Earth-Surface Dynamics). Computa-

tional resources were provided by the Supercomputing Institute for Digital Simulation and Advanced Computation (M SI). J.-F. V inuesa received partial support from a M SI research fellowship.

## References

1. Key, D., 1997, Tropospheric chemistry and transport, *Science* 276, 1043{1047.
2. Schumann, U.: 1989, Large-eddy simulation of turbulent diffusion with chemical reactions in the convective boundary layer, *Atmos. Env.* 23, 1713{1729.
3. Gao, W., Wesely, M. L., Doskey, P. V.: 1993, Numerical modeling of the turbulent diffusion and chemistry of  $\text{NO}_x$ ,  $\text{O}_3$ , isoprene and other reactive trace gases in and above a forest canopy, *J. Geophys. Res.* 98, 18339{18353.
4. Sykes, R. I., Parker, S. F., Henn, D. S., Lewellen, W. S.: 1994, Turbulent mixing with chemical reactions in the planetary boundary layer, *J. Applied Meteorol.* 33, 825{834.
5. Gao, W., Wesely, M. L.: 1994, Numerical modeling of the turbulent fluxes of chemically reactive trace gases in the atmospheric boundary layer, *J. Applied Meteorol.* 33, 835{847.
6. Verver, G. H. L., van Dop, H., Holtslag, A. A. M.: 1997, Turbulent mixing of reactive gases in the convective boundary layer, *Bound.-Layer Meteorol.* 85, 197{222.
7. Molenaker, M. J., Vila-Guerau de Arellano, J.: 1998, Turbulent control of chemical reactions in the convective boundary layer, *J. Atmos. Sci.* 55, 568{579.
8. Petersen, A. C., Beets, C., van Dop, H., Duynkerke, P. G.: 1999, Mass-flux schemes for transport of non-reactive and reactive scalars in the convective boundary layer, *J. Atmos. Sci.* 56, 37{56.
9. Petersen, A. C., Holtslag, A. A. M.: 1999, A first-order closure for covariances and fluxes of reactive species in the convective boundary layer, *J. Appl. Meteorol.* 38, 1758{1776.
10. Petersen, A. C.: 2000, The impact of chemistry on flux estimates in the convective boundary layer, *J. Atmos. Sci.* 57, 3398{3405.
11. Krol, M. C., Molenaker, M. J., Vila-Guerau de Arellano, J.: 2000, Effects of turbulence and heterogeneous emissions on photochemically active species in the convective boundary layer, *J. Geophys. Res.* 105, 6871{6884.
12. Verver, G. H. L., van Dop, H., Holtslag, A. A. M.: 2000, Turbulent mixing and the chemical breakdown of isoprene in the atmospheric boundary layer, *J. Geophys. Res.* 105, 3983{4002.
13. Vila-Guerau de Arellano, J., Cuijpers, J. W. M.: 2000, The chemistry of a dry cloud: the effects of radiation and turbulence, *J. Atmos. Sci.* 57, 1573{1584.
14. Patton, E. G., Davis, K. J., Barth, M. C., Sullivan, P. P.: 2001, Decaying scalars emitted by a forest canopy: a numerical study, *Bound.-Layer Meteorol.* 100, 91{129.
15. V inuesa, J.-F., Vila-Guerau de Arellano, J.: 2003, Fluxes and (co-)variances of reacting scalars in the convective boundary layer, *Tellus* 55B, 935{949.
16. Jonker, H. J. J., Vila-Guerau de Arellano, J., Duynkerke, P. G.: 2004, Characteristic length scales of reactive species in a convective boundary layer, *J. Atmos. Sci.* 61, 41{56.

17. V inuesa, J.-F., Vila-Guerau de Arellano, J.: 2005, Introducing effective reaction rates to account for the inefficient mixing of the convective boundary layer, *Atmos. Env.* 39, 445{461.
18. Moeng, C.H.: 1984, A large-eddy simulation model for the study of planetary boundary-layer turbulence, *J. Atmos. Sci.* 41, 2052{2062.
19. V inuesa, J.-F., Porte-Agel, F.: 2005, A dynamic similarity subgrid model for chemical transformations in Large Eddy Simulation of the atmospheric boundary layer, *Geophys. Res. Lett.* 32, L03814.
20. Porte-Agel, F.: 2004, A scale dependent dynamic model for scalar transport in LES of the atmospheric boundary layer, *Bound.-Layer Meteorol.* 112, 81{105.
21. Meeder, J.P., Nieuwstadt, F.T.M.: 2000, Large-eddy simulation of the turbulent dispersion of a reactive plume from a point source into a neutral atmospheric boundary layer, *Atmos. Env.* 34, 3563{3573.
22. Lilly, D.K.: 1967, The representation of small-scale turbulence in numerical simulation experiments, *Proc. IBM Scientific Computing Symposium on Environmental Sciences*, IBM form no. 320-1951, White Plains, New York, 195{209.
23. Masson, P.J., Derbyshire, S.H.: 1990, Large-eddy simulation of the stably-stratified atmospheric boundary layer, *Bound.-Layer Meteorol.* 53, 117{162.
24. Germano, M.: 1992, Turbulence: the filtering approach, *J. Fluid Mech.* 238, 325{336.
25. Lilly, D.K.: 1992, A proposed modification of the Germano subgrid-scale closure method, *Phys. Fluids A* 4, 633{635.
26. Vila-Guerau de Arellano, J.: 2003, Bridging the gap between atmospheric physics and chemistry in studies of small-scale turbulence, *Bulletin of the American Meteorological Society* 84, 51{56.
27. Pope, S.B.: 2000, *Turbulent flows*, Cambridge University Press.
28. Meneveau, C., Katz, J.: 2000, Scale-invariance and turbulence models for large-eddy simulation, *Rev. Fluid Mech.* 32, 1{32.
29. Albertson, J.D., Parlange, M.B.: 1999, Natural integration of scalar fluxes from complex terrain, *Adv. Wat. Res.* 23, 239{252.
30. Porte-Agel, F., Meneveau, C., Parlange, M.B.: 2000, A scale-dependent dynamic model for large-eddy simulation: application to a neutral atmospheric boundary layer, *J. Fluid Mech.* 415, 261{284.